

FATIGUE FRACTURE OF THE LOGICA CEMENTED STEM – CLINICAL AND MECHANICAL ANALYSIS

Marian Melisik^{1,2}, Peter Palcek³, Libor Necas¹, Martin Zofcak⁴, Michal Al-Khoury¹,
Maros Hrubina^{1,2}

¹University Department of Orthopaedic Surgery, University Hospital Martin, Martin,
Slovak Republic

²Jessenius Faculty of Medicine in Martin, Comenius University in Bratislava, Martin,
Slovak Republic

³Department of Materials Engineering, Faculty of Mechanical Engineering, University of Zilina,
Zilina, Slovak Republic

⁴Department of Orthopaedic Surgery, Hospital Michalovce, Michalovce, Slovak Republic

Abstract

Fracture of a cemented femoral stem is a relatively rare but serious complication of total hip arthroplasty (THA). This study aimed to perform a clinical and biomechanical analysis of six cases of fractured cemented stems to identify the risk factors associated with this type of failure. A retrospective analysis was conducted on six patients with documented stem fractures. Data collected included patient demographics (age, sex, BMI), implant details (stem size, head diameter), and the time from primary surgery to failure. Explanted stems underwent macroscopic evaluation, chemical analysis, and structural assessment using scanning electron microscopy (SEM). All fractured stems were the smallest available sizes (0 or 01) and were paired with XL or XXL femoral heads. The average time from implantation to revision surgery was 88 months (range: 70–102 months). The average BMI was 27.9 kg/m² (range: 20.3–31.1 kg/m²). Macroscopic examination revealed fatigue fractures covering more than 80% of the load-bearing cross-section. Chemical analysis showed that the implants consisted of two distinct materials: the head (AISI 316L steel) and the stem (06Cr18Ni11Nb alloy, AISI 347). Alloy analysis confirmed that the chemical composition largely met standard requirements, except for elevated manganese (Mn) levels and suboptimal niobium (Nb) content, likely due to processing issues. Fractography demonstrated crack initiation in high-stress areas (thread region), with signs of corrosion fatigue and secondary cracking contributing to the failure. Fatigue failure of cemented stems is a rare event. Identified risk factors include small-sized stems combined with larger femoral heads, which increase postoperative offset and biomechanical stress. Material issues, including substandard alloy composition and processing defects, combined with electrochemical interactions between different materials, further predispose these stems to failure.

Keywords

fatigue fracture, cemented stem, total hip arthroplasty, biomechanical analysis

Introduction

Fatigue fractures of cemented femoral stems remain an infrequent but clinically significant complication following total hip arthroplasty (THA). Although the estimated prevalence is low, ranging from 0.02% to 0.68% [1], the impact on the patient is severe, typically necessitating complex revision surgery associated with high morbidity. These failures generally result from

a synergistic interaction between adverse biomechanical loading and the intrinsic material properties of the implant.

Historically, early designs such as the Charnley monoblock stem exhibited fracture rates as high as 4.1%, primarily due to insufficient proximal support and suboptimal cement mantle integrity [2]. While advancements in metallurgy and computer-aided design (CAD) since the 1970s have significantly reduced the incidence of such events [3], contemporary reports

confirm that stem fractures persist in modern clinical practice. Current literature suggests that such failures are frequently linked to localized corrosion at the head-neck junction, manufacturing defects, or specific metallurgical deficiencies [4–6].

In our clinical practice, we identified six cases of fatigue failure involving the cemented Logica stem (LimaCorporate, Udine, Italy). Preliminary observations suggest multifactorial etiology. We hypothesize that the combination of small-sized stems with larger femoral heads and increased offsets creates a detrimental lever arm, significantly elevating the bending moments acting on the femoral component. This mechanical stress may be further compounded by material inconsistencies and manufacturing factors that compromise the long-term structural integrity of the alloy.

The objective of this study was to provide a comprehensive analysis of these six failure cases from both a biomechanical and a material science perspective. Utilizing advanced diagnostic techniques, including scanning electron microscopy (SEM) and microhardness testing, we aimed to elucidate the underlying failure mechanisms and identify specific risk factors. The findings were compared with current literature to provide broader insights into the prevention of fatigue-related complications in cemented THA.

Materials and methods

Study Design and Patient Population

This retrospective observational study evaluated six patients who sustained a fracture of a cemented. Clinical and demographic data—including age, sex, body mass index (BMI), surgical details, and radiographs—were retrieved from the Slovak Arthroplasty Register [7]. All patients provided informed consent for the use of their data for research purposes. The parameters analyzed included stem size, femoral head diameter, and the time interval from primary surgery to implant failure.

Radiological Analysis

Postoperative and pre-revision radiographs were independently reviewed to assess the mechanical environment of the implant. The following parameters were measured:

Stem Alignment: The orientation of the stem within the femoral canal was categorized as neutral, varus, or valgus.

Femoral Offset: Medial-lateral reconstruction was evaluated to determine the postoperative offset and its potential influence on the lever arm.

Cement Mantle Thickness: The integrity and thickness of the polymethylmethacrylate (PMMA) layer were assessed in accordance with Barrack's grading

system, focusing on the proximal and mid-stem regions to identify areas of potential debonding or insufficient support [8].

Implant Characteristics

The Logica cemented stem features a polished, tapered design manufactured from a nitrogen-strengthened austenitic stainless-steel alloy (FeCrNiMnMoNbN) compliant with the ISO 5832-1 standard. The implants analyzed in this study featured a 12/14 mm Eurocone taper and were primarily the smaller size variants (0 and 01).

Chemical Analysis

To verify material composition and identify deviations from the EN 10088-1 (06Cr18Ni11Nb) standard, chemical analysis was performed on both the stem and the femoral head.

Method: Elemental composition was determined via optical emission spectrometry (OES) using a SPECTROMAXx (Germany) spectrometer.

Procedure: Three measurements were taken per sample across the stem cross-section and the head surface. Surfaces were mechanically ground and degreased with ethanol prior to analysis to ensure precision SEM and fractography. A detailed fractographic analysis was conducted to differentiate between fatigue and corrosion-related failure mechanisms.

Instrumentation: A TESCAN VEGA II field-emission SEM was utilized.

Imaging Conditions: Analysis was performed using secondary electron (SE) and back-scattered electron (BSE) detectors at an accelerating voltage of 30 kV. Magnification ranged from 20× to 5000×.

Criteria: Fatigue failure was identified by macroscopic beach marks (rest lines) and microscopic fatigue striations. Corrosion-related features were defined by intercrystalline facets and secondary cracks.

Sample Preparation: Surfaces were cleaned ultrasonically in acetone and ethanol. For microstructural assessment, samples were cross-sectioned, metallographically polished, and etched with Vilella's reagent to reveal grain boundaries and carbide distribution.

Microhardness Testing

To evaluate the homogeneity of mechanical properties and potential work hardening, Vickers microhardness was measured.

Method: Tests were performed according to ISO 6507-1 (HV 0.5) using a 500 g (4.903 N) load and a 10-second dwell time.

Procedure: A series of 22 indents were made from the outer surface to the core, with 250 µm spacing to prevent strain field interference.

Table 1: Basic demographic characteristics of the group of patients with broken Logica stem.

Patient	Gender	Age (years)	Time since primary implantation (years)	Weight (kg)	BMI	Size of the stem	Size of the head
1	F	76	8.2	82	30.1	01	M
2	F	86	8.5	83	29.0	0	XL
3	F	79	8.1	79	29.2	01	XXL
4	F	85	6.0	88	31.1	0	XL
5	M	78	5.8	65	20.3	01	XXL
6	F	73	7.3	78	27.5	01	XL

Tensile Strength Estimation: Local ultimate tensile strength (R_m) was estimated using the empirical formula $R_m \approx 3.2 \times HV$, which is consistent with ISO 18265 approximations for austenitic steels.

Statistical Analysis

Descriptive statistics were used to summarize patient demographics and hardness distribution. Measurement uncertainty for chemical analysis was maintained within a $\pm 5\%$ plus confidence interval.

Results

Clinical Analysis

From April 2008 to April 2023, a total of 1,354 Logica stems of various sizes were recorded in our registry [7]. The combination of stem sizes 0 and 01 with XL or XXL heads was utilized in 40 cases. The overall revision rate for the entire cohort was 3.32%, including six specific cases (0.44%) of stem fracture. This fracture cohort consisted of five women and one man, with a mean age of 79.5 years (range 73–86, SD 4.76) and a mean BMI of 27.9 (range 20.3–31.1, SD 3.96). The average time from primary surgery to fracture detection was approximately 88 months (range 70–102, SD 2.35) (Tab. 1).

All patients reported sudden, severe pain and an immediate inability to bear weight without preceding trauma.

Radiological analysis

Stem Alignment: All six implants (100%) were positioned in neutral alignment within the femoral canal; no varus or valgus deviations were observed.

Cement Mantle Thickness: The PMMA layer demonstrated consistent thickness ranging from 2 to

3 mm in the proximal and mid-stem regions. According to Barrack's grading system [8], the mantle was intact and provided adequate circumferential support.

Femoral Offset: Medial-lateral reconstruction values were maintained between 28 and 32 mm, ensuring a consistent lever arm across all cases. The postoperative offset was higher than preoperative in every case.

Implant Stability: No radiographic signs of loosening, such as progressive radiolucent lines or osteolysis, were identified in any of the fractured stems prior to failure. This suggests that the implants remained rigidly fixed within the cement mantle until the point of mechanical failure.

Radiographs confirmed the fractures in all instances (Fig. 1).



Fig. 1: The anteroposterior X-ray of 79-year-old patient with broken cemented stem Logica 8 years after the implantation.

All fractured stems were the smallest available sizes (0 or 01) and were paired with XXL or XL heads. During revision surgery, a modular revision stem was implanted in four cases following endofemoral cement removal. In

two cases, a "cement-in-cement" technique with a new stem of the same size was performed to minimize operative time in elderly, polymorbid patients. The recurrence of fractures exclusively in the smallest stem sizes combined with long-neck heads (XL, XXL) suggests a potential correlation between slender implant geometry, increased offset, and elevated mechanical stress (Fig. 2).



Fig. 2: The endoprosthesis head with visible XXL label.

Mechanical and Material Analysis

Macroscopic evaluation revealed that fracture initiation occurred in the thread region, subsequently propagating through the entire cross-section (Fig. 3–5).



Fig. 3: Fractured Logica stem, explanted component.

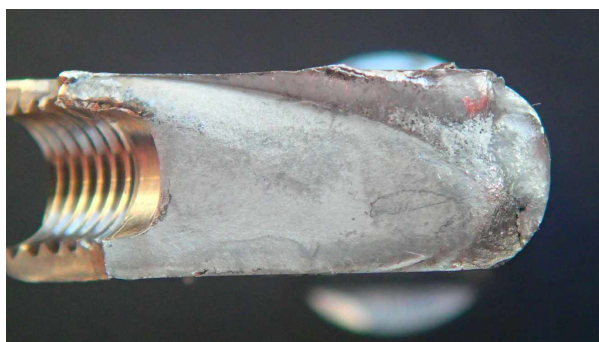


Fig. 4: Fracture surface morphology of the proximal (upper) part of the broken femoral stem.



Fig. 5: Fracture surface morphology of the distal (lower) part of the broken femoral stem.

Chemical analysis identified a multi-material assembly: the head was composed of AISI 316L stainless steel, whereas the stem consisted of AISI 347 (06Cr18Ni11Nb). While the primary alloying elements (C, Cr, Ni, Mo) generally adhered to standard specifications, manganese (Mn) levels were elevated, and niobium (Nb) content was below the nominal range. SEM identified a high density of *M23C6* carbides precipitated at the grain boundaries. Fractographic analysis confirmed crack initiation at high-stress concentrations (threads), characterized by fatigue striations and secondary cracks. Additionally, evidence of corrosion damage was observed on the fracture surface.

Microhardness and Tensile Strength Estimation

Microhardness testing (HV0.5) revealed a non-uniform distribution ranging from 315 to 370 HV. To assess the mechanical implications, the local ultimate tensile strength (R_m) was estimated using the empirical conversion $R_m \approx 3.2 \times HV$, a standard approximation for austenitic stainless steels. Based on this relationship, the observed hardness variation of 55 HV corresponds to a local strength fluctuation of approximately 150–170 MPa. Each data point represents the mean of five indents (HV0.5) per location; measurement variability remained low, with a standard deviation typically within ± 5 HV.

Failure Characteristics and Microstructural Interpretation

The fracture morphology is consistent with fatigue failure. The presence of grain-boundary *M23C6* carbides suggests susceptibility to intergranular corrosion, which, under cyclic physiological loading, likely accelerated the degradation process (Fig. 6).

The microhardness profile, peaking near the surface, suggests strain hardening induced during the final mechanical polishing. In contrast, core hardness fluctuations may indicate non-homogeneous heat treatment (e.g., suboptimal solution annealing) following forging (Fig. 7).

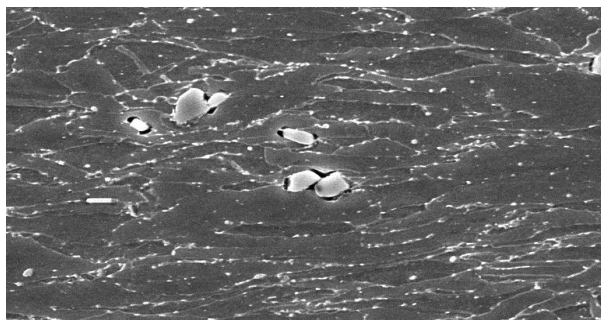


Fig. 6: Microstructure of the fractured stem highlighting grain-boundary carbides associated with fatigue failure and intergranular corrosion.

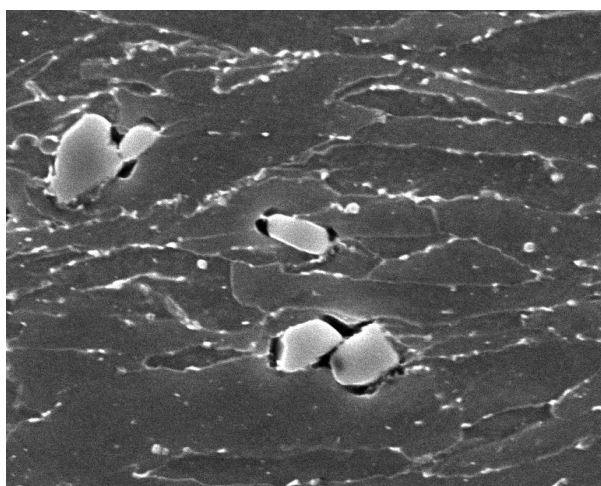


Fig. 7: Microstructural detail showing M23C6 carbides and grain morphology relative to the microhardness profile.

Furthermore, the presence of corrosion products on the fracture surface suggests a potential galvanic effect between the dissimilar metals (AISI 316L and AISI 347), acting synergistically with mechanical fatigue in the aggressive biological environment (Fig. 8).

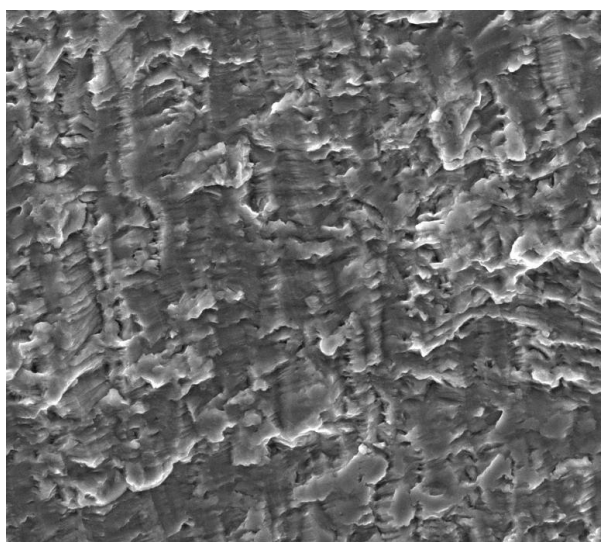


Fig. 8: SEM micrograph of the fatigue fracture cross-section showing typical fatigue striations and localized corrosion products.

Figure 9 provides a schematic showing the cross-section of the femoral stem and the measurement line along which hardness values were collected, starting from the outer surface towards the center axis. The areas of cross-sections were identical at in work of Cubillos et al. [9] (Fig. 9).

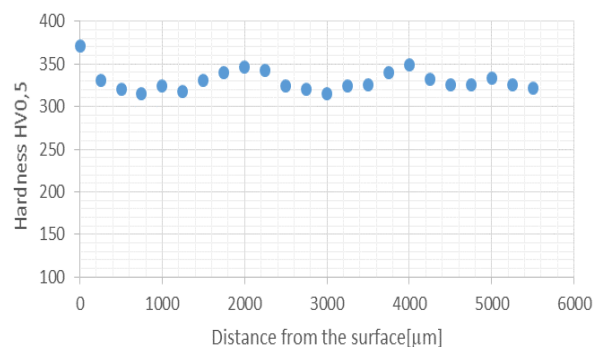


Fig. 9: Microhardness profile across the femoral stem cross-section. Data points represent mean values from six fractured stems, measured along a radial path from the outer surface to the central axis.

Discussion

Femoral stem fracture after THA remains a rare but severe complication, with a reported prevalence between 0.02% and 0.68% [10–14]. Our analysis of six fractured stems confirms that failure resulted from a synergistic interplay between unfavorable geometric configurations, metallurgical deficiencies, and electrochemical degradation.

Biomechanical and Geometric Risk Factors

A critical observation in this cohort was that all failures occurred in the smallest available stem sizes (0 and 01) when combined with extended femoral heads (XL or XXL). This specific configuration significantly increases the lever arm, thereby drastically amplifying the cantilever bending moments. Radiographically, the stems exhibited neutral alignment and a robust cement mantle (2–3 mm). This rigid fixation, while clinically stable, likely concentrated the entire mechanical load onto the small cross-section of the implant. The absence of radiographic loosening confirms that the failure was not initiated by clinical instability but by a detrimental biomechanical environment that exceeded the material's fatigue limit.

Fractographic and Metallurgical Evidence

Fractographic analysis via SEM provided definitive evidence of the failure mode. The crack initiation sites were consistently located in the high-stress thread regions. The presence of fatigue striations, rest lines, and secondary cracking confirms that fatigue failure was the

primary mechanism, accounting for over 80% of the fracture cross-section. This mechanical vulnerability was compounded by material inconsistencies. Chemical analysis revealed significant deviations from the ISO 5832-1 standard, specifically elevated manganese (Mn) levels and fluctuating niobium (Nb) content in the AISI 347 stem alloy. The observed *M23C6* carbide precipitation at grain boundaries and microhardness fluctuations (315–370 HV) suggest suboptimal solution annealing. These metallurgical defects likely increased the material's susceptibility to intergranular corrosion, facilitating crack initiation under cyclic loading.

Electrochemical Interaction

Furthermore, the use of chemically distinct materials—an AISI 316L head paired with an AISI 347 stem—created a potentially galvanic cell. In the aggressive physiological environment, this interaction may have acted as a secondary driver for corrosion fatigue, a mechanism previously implicated in high-profile recalls of other modular systems.

Limitations

This study is limited by its small sample size ($n=6$) and the lack of direct tensile testing, necessitating the use of empirical strength estimations. Despite these limitations, the consistency of the fractographic and chemical findings provides strong evidence for the identified failure mechanisms.

Conclusion

The fatigue fracture of the cemented Logica stem is a complex failure mechanism driven by the synergy of biomechanical and material factors. These findings underscore the necessity for meticulous preoperative planning, particularly for patients with a high BMI. Surgeons should exercise extreme caution when combining small-sized cemented stems with high-offset heads, as the resulting bending moments may surpass the fatigue strength of the material.

Acknowledgement

The work received no external funding.

Ethical review and approval were waived for this study due to retrospective analysis of the data and imaging results of patients. This retrospective review study involving human participants was in accordance with the ethical standards of the institutional and national research committee and with the 1964 Helsinki Declaration and its later amendments or comparable ethical standards.

The authors declare no conflict of interest.

References

- [1] Turnbull GS, Soete S, Akhtar MA, Ballantyne JA. Risk factors for femoral stem fracture following total hip arthroplasty: a systematic review and meta analysis. *Archives of Orthopaedic and Trauma Surgery*. 2024;144(5):2421–8. DOI: [10.1007/s00402-024-05281-x](https://doi.org/10.1007/s00402-024-05281-x).
- [2] Dall DM, Learmonth ID, Solomon MI, Miles AW, Davenport JM. Fracture and loosening of Charnley femoral stems. *The Journal of Bone & Joint Surgery British Volume*. 1993;75(2):259–65. DOI: [10.1302/0301-620X.75B2.8444947](https://doi.org/10.1302/0301-620X.75B2.8444947).
- [3] Sudhakar KV, Wang J. Fatigue behavior of Vitallium-2000 Plus alloy for orthopedic applications. *Journal of Materials Engineering and Performance*. 2011;20(6):1023–8. DOI: [10.1007/S11665-010-9716-Z](https://doi.org/10.1007/S11665-010-9716-Z).
- [4] Hrubina M, Behounek J, Skotak M. Mid-term results of cementless ultima cups in primary total hip replacement. *Acta Chirurgiae Orthopaedicae et Traumatologiae Cechoslovaca*. 2008;75(3):205–11. DOI: [10.55095/achot2008/039](https://doi.org/10.55095/achot2008/039).
- [5] Lee EW, Kim HT. Early fatigue failures of cemented, forged, cobalt-chromium femoral stems at the neck-shoulder junction. *The Journal of Arthroplasty*. 2001;16(2):236–8. DOI: [10.1054/arth.2001.20542](https://doi.org/10.1054/arth.2001.20542).
- [6] Murphy SB, Rodriguez J. Revision total hip arthroplasty with proximal bone loss. *The Journal of Arthroplasty*. 2004;19(4):115–9. DOI: [10.1016/j.arth.2004.04.001](https://doi.org/10.1016/j.arth.2004.04.001).
- [7] Slovak Arthroplasty Register (SAR) [Internet]. Available from: <https://sar.mfn.sk/>.
- [8] Barrack RL, Mulroy RD, Harris WH. Improved cementing techniques and femoral component loosening in young patients with hip arthroplasty. A 12-year radiographic review. *The Journal of Bone & Joint Surgery British Volume*. 1992;74(3):385–9. DOI: [10.1302/0301-620X.74B3.1587883](https://doi.org/10.1302/0301-620X.74B3.1587883).

- [9] Cubillos PO, dos Santos CT, dos Santos VO, Caminha IM, da Rosa E, Roesler CR. A proposition to standardize the microstructural grain size measurements of hip stems. *Journal of Testing and Evaluation*. 2021;49(2):1412–22. DOI: [10.1520/JTE20190038](https://doi.org/10.1520/JTE20190038)
- [10] Bäcker HC, Wu CH, Kienzle A, Perka C, Gwinner C. Mechanical failure of total hip arthroplasties and associated risk factors. *Archives of Orthopaedic and Trauma Surgery*. 2023;143(2):1061–9. DOI: [10.1007/s00402-022-04353-0](https://doi.org/10.1007/s00402-022-04353-0).
- [11] Panzures A, Faisal S, Sivakumar A, Kazmi SA, Turnbull G, Ballantyne A, et al. Evaluating the risk factors for Lubinus SP II femoral stem fractures: A case series of 5 primary total hip arthroplasty patients with a mean follow-up of 7.5 years. *Sage Open Medical Case Reports*. 2025;13: 2050313X251366366. DOI: [10.1177/2050313X251366366](https://doi.org/10.1177/2050313X251366366).
- [12] Heck DA, Partridge CM, Reuben JD, Lanzer WL, Lewis CG, Keating EM. Prosthetic component failures in hip arthroplasty surgery. *The Journal of Arthroplasty*. 1995;10(5):575–80. DOI: [10.1016/s0883-5403\(05\)80199-8](https://doi.org/10.1016/s0883-5403(05)80199-8).
- [13] Al Habsi S, Luthra JS, Al Badei H. Taper fracture of Uncemented femoral stem after total hip arthroplasty. *Case Reports in Orthopedic Research*. 2018;1(1):50–4. DOI: [10.1159/000495359](https://doi.org/10.1159/000495359).
- [14] Wylde CH, Jenkins E, Pabbruwe M, Bucher T. Catastrophic failure of the Accolade I hip arthroplasty stem: a retrieval analysis study. *Hip International*. 2020;30(4):481–7. DOI: [10.1177/1120700020919665](https://doi.org/10.1177/1120700020919665).

*Assoc. prof. Maros Hrubina, MD., Ph.D.
Department of Orthopaedic Surgery
University Hospital Martin
Kollarova 2, 036 59, Martin
Slovak Republic*

*E-mail: mhrubina@gmail.com
Phone: +421 908 616 368*